

# Fe<sub>2</sub>O<sub>3</sub>/Al<sub>2</sub>O<sub>3</sub> catalysts for the N<sub>2</sub>O decomposition in the nitric acid industry

Grzegorz Giecko<sup>a,\*</sup>, Tadeusz Borowiecki<sup>a</sup>, Wojciech Gac<sup>a</sup>, Janusz Kruk<sup>b</sup>

<sup>a</sup> Department of Chemical Technology, Faculty of Chemistry, University of Maria Curie-Skłodowska, M. Curie-Skłodowska Sq. 3, 20-031 Lublin, Poland

<sup>b</sup> Institute of Fertilizers, 24-100 Puławy, Poland

Available online 25 March 2008

## Abstract

Fe<sub>2</sub>O<sub>3</sub> catalysts supported on Al<sub>2</sub>O<sub>3</sub> were used to remove nitrous oxide from the nitric acid plant simulated process stream (containing O<sub>2</sub>, NO and H<sub>2</sub>O). Catalysts were prepared by the coprecipitation method and were characterized for their physico-chemical properties by BET, XRD, AFM and TPR analysis. A strong influence of the post-preparation heating conditions on the structural and catalytic properties of the catalysts has been evidenced. Laboratory tests revealed 95% conversion of N<sub>2</sub>O at temperature 750 °C and a slight decrease in activity in the presence of H<sub>2</sub>O and NO. The catalysts were inert towards decomposition of NO. The pilot-plant reactor and real plant studies (up to 3300 h time-on-stream) confirmed high activity and very good mechanical stability of the catalysts as well as no decomposition of nitric oxide.

© 2008 Elsevier B.V. All rights reserved.

**Keywords:** Nitrous oxide; Decomposition; Nitric acid; Abatement; Iron catalysts

## 1. Introduction

The main anthropogenic activities producing N<sub>2</sub>O are agricultural soil management, fuel combustion in motor vehicles, nitric acid production, stationary fuel combustion, manure management and wastewater treatment. N<sub>2</sub>O has been considered as one of the largest contributor to the global anthropogenic greenhouse gas emissions which is over 300 (global warming potential (GWP) is 310 in 100 years time horizon) times more effective than CO<sub>2</sub> in trapping heat in the stratosphere [1]. Nitric acid production is the largest industrial source of nitrous oxide where N<sub>2</sub>O is produced as an unwanted by-product of the catalytic oxidation of ammonia. Nitrous oxide abatement from nitric acid plants is one of the most challenging environmental problems in catalysis.

Besides the improvement/optimization of ammonia oxidation catalysts there are three possible options for catalytic decomposition of N<sub>2</sub>O in the nitric acid plant. Firstly, the catalysts can be used in the ammonia oxidation chamber just downstream of the NH<sub>3</sub> oxidation catalyst. The second abatement measures remove N<sub>2</sub>O from the tail-gas leaving the absorption column before the expander. The third option,

typical end-of-pipe, is to decompose N<sub>2</sub>O in a tail-gas downstream of the expander [2–5]. Most of the studies presented in the literature deal with the catalysts for nitrous oxide decomposition for the second and third abatement method because of the mild reaction conditions (temperature between 100 and 500 °C at pressures of 1–12 bar).

This paper concerns the first location of the catalysts which is one of the most promising among the several N<sub>2</sub>O abatement methods, but it demands a high stability of the catalyst and a very high selectivity for N<sub>2</sub>O decomposition since destruction of NO is unacceptable in the production process. Numerous N<sub>2</sub>O decomposition catalysts are known and most of these are based on various metal oxides [5,6] very often supported on zeolite carriers or in the form of metal ion exchanged zeolites [7–12]. However, the practical use of these zeolitic systems in the ammonia oxidation chamber is likely to be problematic due to their deactivation under hydrothermal conditions. Iron zeolites are often used as catalysts for low-temperature tail-gas removal of N<sub>2</sub>O with reductants [5]. A reducing agent (methane, propane, LPG and ammonia) is added to the tail-gas leaving the NO<sub>2</sub> absorber. Hydrocarbons are widely used as reductants and CH<sub>4</sub> is considered as one of the most efficient among them [13,14]. Depending on the type of the reductant, the catalyst used and the reaction conditions the co-addition of hydrocarbon powers the temperature for N<sub>2</sub>O reduction over iron zeolites around 100 °C with respect to direct N<sub>2</sub>O

\* Corresponding author. Tel.: +48 81 5375526; fax: +48 81 5375565.

E-mail address: [ggiecko@hermes.umcs.lublin.pl](mailto:ggiecko@hermes.umcs.lublin.pl) (G. Giecko).

decomposition [5]. One of the commercially implemented processes of  $\text{N}_2\text{O}$  removal using iron-containing zeolites in the presence of  $\text{NH}_3$  and  $\text{CH}_4$  is Uhde EnviNOx [13].

Most of the efforts to develop catalysts suitable to use in a nitric acid production plant have been made by the companies [15–19]. Among the most promising are the catalysts based on cobalt-oxide spinels (composition  $\text{Co}_{3-x}\text{M}_x\text{O}_4$ , where  $\text{M}=\text{Fe}$ ,  $\text{Al}$  and  $x = 0\text{--}2$ ) supported on cerium oxide developed by Norsk Hydro [20].  $\text{Co}_2\text{AlO}_4/\text{CeO}_2$  catalyst with the addition of  $\text{ZrO}_2$  (0.2 wt.%) showed exceptional activity in decomposing  $\text{N}_2\text{O}$  (over 95%) and stability in the real-plant conditions. The catalyst can be used at a wide temperature range and is stable at varying gas composition, even in the presence of relatively high amounts of water, which often is a problem. Furthermore,  $\text{NO}$  losses in the real-plant tests occurred to be lower than 0.2%.

The main objective of this paper was to arrive at a versatile, active and thermally stable catalyst for  $\text{N}_2\text{O}$  decomposition at extreme conditions of the ammonia oxidation process with high selectivity for decomposing nitrous oxide without decomposing  $\text{NO}$ .

## 2. Experimental

### 2.1. Catalysts preparation

$\text{Fe}_2\text{O}_3/\text{Al}_2\text{O}_3$  catalysts series were prepared by coprecipitation using the aqueous solutions of iron (III) nitrate and alumina (III) nitrate with sodium (II) hydroxide at different pH of solutions (8.5 and 9.5). The catalysts were dried after precipitation at  $105^\circ\text{C}$  for 24 h and then calcined at  $400^\circ\text{C}$  for 4 h. Afterwards samples were heated at  $900^\circ\text{C}$  or at  $1100^\circ\text{C}$  for 5 h to simulate the catalyst aging and reactor exotherms. For the pilot-plant studies catalysts were formed in  $17\text{ mm} \times 17\text{ mm} \times 12\text{ mm}$  Raschig rings and  $5\text{ mm} \times 5\text{ mm}$  pellets.

### 2.2. Catalysts characterization

The chemical composition of the samples was determined by applying the X-ray fluorescence method (ED-XRF Canbera 1510). The total surface area of the samples was determined by measuring argon adsorption at the temperature of liquid nitrogen in a static-volumetric apparatus, which ensured a vacuum better than  $2 \times 10^{-6}\text{ kPa}$ . X-ray diffraction studies (XRD) were done in the HZG-4 diffractometer using  $\text{Cu K}\alpha$  radiation ( $\lambda = 1.5418\text{ \AA}$ ). The morphology of the samples was studied by the atomic force microscopy (AFM) using Nanoscope III (Digital Instruments) microscope.

The temperature-programmed reduction was carried out in the Altamira AMI-1 system. The 0.02–0.05 g catalysts samples (with the grain size equal to 0.2–0.5 mm) were introduced into the quartz reactor (i.d. = 7 mm). A temperature controller maintained the reactor temperature within  $1^\circ\text{C}$  and provided linear temperature programming. The monitoring of the gas composition was followed by means of a mass spectrometry detector HAL 201 RC (Hidden Analytical). During TPR measurements an  $\text{LN}_2$ -methanol trap was placed between the

reactor and detector to remove water. In the TPR measurements 6 vol.%  $\text{H}_2$  in Ar mixture was applied. The gases were of 99.995% purity and were further purified by OXICLEAR or  $\text{MnO}/\text{SiO}_2$  traps.

### 2.3. Activity tests

Catalytic tests were carried out in a tubular quartz reactor using 0.1 g of catalysts shaped in particles with diameters of 0.63–1 mm. The tests were carried out at the atmospheric pressure in the model mixture of gases formed in the ammonia oxidation chamber in the nitric acid plant. The partial pressure of the gases was 5–10 mbar for  $\text{N}_2\text{O}$ , 5–10 mbar for  $\text{O}_2$ , 30 mbar  $\text{NO}$ , 30–60 mbar for  $\text{H}_2\text{O}$ , balance He at different gas mixture compositions. The total flow of the reactant gases amount to 50 or  $100\text{ cm}^3/\text{min}$ . Individual and combined effects of these gas mixtures on the catalytic performance were investigated. All the samples were heated at  $900^\circ\text{C}$  for 1 h in flowing helium prior to reaction and cooled down in the same gas to the reaction temperature. The reaction temperatures ranged from the ambient up to  $800^\circ\text{C}$ . The products were continuously analyzed by a mass spectrometer (Hidden Analytical HAL201RC) and discontinuously by GC (Fisons GC8000) equipped with the thermal conductivity detector using a Porapak Q 100/120 mesh column. At least three analyses for the GC were averaged for a data point.

Pilot-plant tests were carried out in the three-reactor system. The reactor construction was the same as an industrial one made up from Pt–Rh gauzes and the bed of ceramic Raschig rings in the reference reactor or the catalyst in experimental reactors. Each reactor was fed with the same gas mixture containing 10.7 vol.% of  $\text{NH}_3$  in air at the flow rate  $45\text{ Nm}^3/\text{h}$  (conditions the same as in the real plant). The reaction was carried out at 4.9 bars pressure and at the temperature range  $885\text{--}890^\circ\text{C}$ . The measured  $\text{N}_2\text{O}$  concentration (in the reference reactor) was 1200–1300 ppm.

The catalysts were also placed in the real plant ammonia oxidation reactor (ZA “Pulawy”) for 3300 h and then characterized for the mechanical stability and activity towards  $\text{N}_2\text{O}$  decomposition.

## 3. Results

### 3.1. The physico-chemical properties of the catalysts

The catalysts were prepared by a coprecipitation method using different amounts of solutions at different pH of the ones. Table 1 shows the composition and total surface area of the samples. The assumption of the preparation step was to prepare series of the catalysts with different Fe/Al ratios. In order to obtain an aging effect, post-preparation thermal treatment of the samples was used. The catalysts are denoted as  $\text{FeAl}_x\text{-T}_y$  where  $x$  stands for Fe/Al molar ratio in the samples and  $y$  stands for the temperature of post-preparation heating in degrees of Celsius.

The higher thermal treatment of the samples the lower total surface area of the ones.

Table 1  
Composition and surface properties of the samples

Catalyst	Composition (wt.%)		Post-preparation heating, 5 h (°C)	pH of coprecipitation solution	$S_{\text{BET}}$ (m <sup>2</sup> /g)
	Fe <sub>2</sub> O <sub>3</sub>	Al <sub>2</sub> O <sub>3</sub>			
FeAl <sub>3.5</sub> -T <sub>1100</sub>	72.6	27.4	1100	9.5	3.4
FeAl <sub>3.5</sub> -T <sub>900</sub>	72.4	27.6	900	9.5	11.6
FeAl <sub>3.0</sub> -T <sub>1100</sub>	69.9	30.1	1100	8.5	4.8
FeAl <sub>3.0</sub> -T <sub>900</sub>	68.6	31.4	900	8.5	8.3
FeAl <sub>1.0</sub> -T <sub>1100</sub>	42.8	57.2	1100	9.5	4.8
FeAl <sub>1.0</sub> -T <sub>900</sub>	41.8	58.2	900	8.5	19.9

Fig. 1 shows XRD curves of the samples after calcination at 400 °C and heating at 900 or 1100 °C. The curves for all the samples showed very clearly the presence of the well defined, low dispersed crystalline Fe<sub>2</sub>O<sub>3</sub> rhombohedral phase with the highest intensity of reflections at  $2\theta = 33\text{--}36^\circ$ . This is the only phase observed for the FeAl<sub>3.0</sub> catalysts. Despite the larger amount of Fe<sub>2</sub>O<sub>3</sub> for the catalysts of series FeAl<sub>3.5</sub> the presence of the highly dispersed  $\alpha$ -Al<sub>2</sub>O<sub>3</sub> phase can be seen in XRD curves (reflection peaks located at angles  $25.6^\circ$ ,  $43^\circ$ ,  $52.6^\circ$  and

$57.6^\circ$ ). This fact points to the importance of the pH level during the precipitation of the catalysts precursors.

The confirmation of these results is in the analysis of the XRD patterns for FeAl<sub>1.0</sub> catalysts. These samples contain both Fe<sub>2</sub>O<sub>3</sub> as well as the  $\alpha$ -Al<sub>2</sub>O<sub>3</sub> rhombohedral phase but the intensity of the peaks corresponding to alumina oxide are lower for the sample prepared from the solution of lower pH. The lack of changes in the peak shape or intensity for other heated catalysts indicates that these changes did not come out from

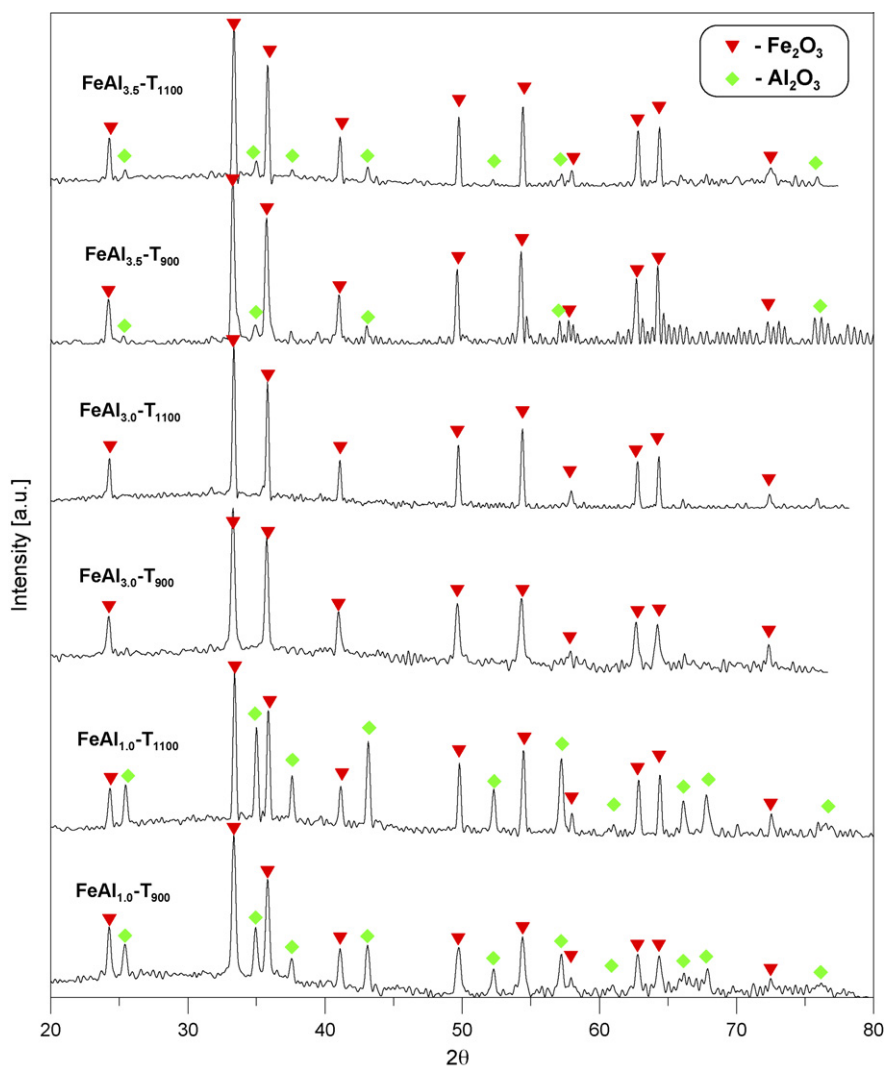


Fig. 1. XRD curves of the catalysts.

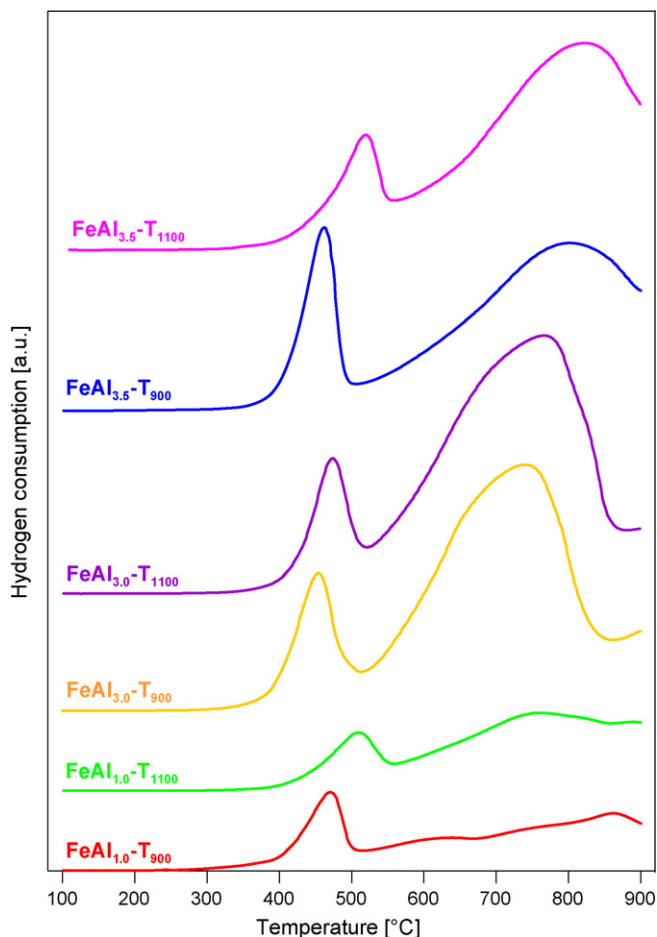


Fig. 2. Temperature programmed reduction curves of the catalysts.

post-preparation heating of the samples. These results are in a good agreement with the TPR (temperature-programmed reduction) experiments data (Fig. 2) which clearly show the presence of this type of oxide forms at the surface of the catalysts.

$\text{Fe}_2\text{O}_3$  in the catalysts was reduced in two-step process via  $\text{Fe}_3\text{O}_4$  [21,22]. The TPR results for the FeAl catalysts showed clearly a presence of two main ranges of the reduction process. The first one at  $T = 450\text{--}530\text{ }^\circ\text{C}$  reveals the presence of  $\text{Fe}_2\text{O}_3$  oxides and the second one, the relatively wide reduction stage at  $T = 750\text{--}850\text{ }^\circ\text{C}$  corresponding to the presence of bulk  $\text{Fe}_3\text{O}_4$  and iron aluminates ( $\text{FeAl}_2\text{O}_4$ ). The reduction peaks are shifted to the higher temperatures for the samples heated at  $1100\text{ }^\circ\text{C}$ . This indicates the formation of hardly reducible species due to a high-temperature sintering process.

Atomic force microscopy (AFM) pictures showed clearly the influence of the temperature post-treatment of the catalysts on their surface properties. The higher temperature of heating the larger average size of the particles thus the smaller total surface area of the catalysts (Fig. 3).

### 3.2. Activity results

Laboratory tests showed, that all catalysts exhibited the activity in the  $\text{N}_2\text{O}$  decomposition reaction. Catalysts were also inactive in the NO decomposition up to  $800\text{ }^\circ\text{C}$ . The presence of

oxygen in the feed does not influence the catalysts activity so the results for the reaction mixture (1 vol.% of  $\text{N}_2\text{O}$  in He) are not shown. Fig. 4 shows the catalysts activity in the presence of NO and  $\text{O}_2$  in the reaction mixture.

The differences in the  $\text{N}_2\text{O}$  conversion between the most and less active samples at higher temperatures ( $>700\text{ }^\circ\text{C}$ ) were over 40%. Fig. 5 shows conversion results at different reaction mixture compositions with comparison to the total surface area of the samples at  $T = 750\text{ }^\circ\text{C}$ .

The addition of  $\text{H}_2\text{O}$  affects the activity of all catalysts used for the  $\text{N}_2\text{O}$  decomposition. The presence of small amount of water vapour (3 vol.%) changes slightly the  $\text{N}_2\text{O}$  conversion (decrease up to 5%) while the higher water vapour concentration (6 vol.%) severely inhibits the reaction (decrease in conversion up to 10–30%). The presence of NO surprisingly decreases the activity of the catalysts which is in contrast to the results reported by Pérez-Ramírez et al. [23] for the Fe catalysts supported on zeolites. The most active catalyst ( $\text{FeAl}_{1.0}\text{-T}_{900}$ ) is also the most resistant for the reaction mixture conditions. There is a good correlation between the reactivity and the total surface area of the samples. This indicates strong relationships between the preparation conditions (mainly the temperature aging process) thus surface properties and the activity of the catalysts. There is no direct correlation between the composition of the catalysts (i.e. Fe/Al ratio) and their activity.

The pilot-plant tests were carried out in the three-reactor system showed in the picture (Fig. 6). All of the reactors contained the Pt–Rh gauzes and a bed of Raschig rings.

First reactor simulated work of a typical ammonia oxidation chamber. In the second and third reactor the inert Raschig rings were substituted with catalysts. The catalyst in the shape of Raschig rings was used in the second reactor and in the shape of pellets in the third one. Fig. 7 shows the results of pilot-plant experiments for one of the FeAl catalysts (called WT-1, properties of which are not shown here due to the ongoing patent application).

The results in the real conditions showed the  $\text{N}_2\text{O}$  conversion over 70%. We can assume that in the real plant reactor the  $\text{N}_2\text{O}$  decomposition level can be higher due to the thicker catalyst bed. In our experiment the catalyst bed had a height of 56 mm while in the real-plant reactor it can be 300 mm. The stability of the sample aged at  $1100\text{ }^\circ\text{C}$  was better (no decrease in conversion during experiment) than for the catalyst heated at  $900\text{ }^\circ\text{C}$ . There were almost no changes in the  $\text{NH}_3$  conversion to NO (we observed even a small increase, up to 0.5%, in the level of conversion) as well as no decrease in the NO concentration in the post-process gas. The WT-1 catalyst was also placed in the real-plant ammonia oxidation reactor, under the Pt–Rh gauzes for 3300 h. After that time the mechanical stability tests revealed almost no changes in the perpendicular flattening resistance of the sample comparing to the fresh one. The activity tests towards the  $\text{N}_2\text{O}$  decomposition for this catalyst showed the level of conversion similar to that obtained in the pilot-plant experiments after 180 h of work. This fact points to very good mechanical resistance of these catalysts. The activity of the catalysts (the  $\text{N}_2\text{O}$  conversion  $\sim 70\%$ ) in the pilot plant experiment is similar to the results reported by BASF company



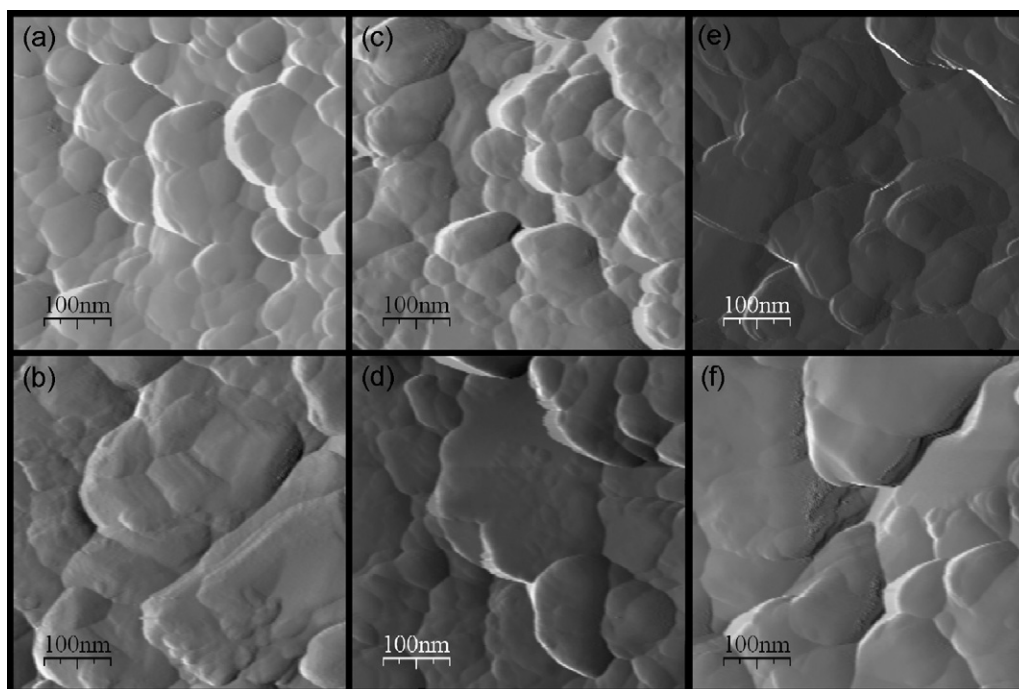


Fig. 3. AFM images of the catalysts (a)  $\text{FeAl}_{1.0}\text{-T}_{900}$ , (b)  $\text{FeAl}_{1.0}\text{-T}_{1100}$ , (c)  $\text{FeAl}_{3.0}\text{-T}_{900}$ , (d)  $\text{FeAl}_{3.0}\text{-T}_{1100}$ , (e)  $\text{FeAl}_{3.5}\text{-T}_{900}$  and (f)  $\text{FeAl}_{3.5}\text{-T}_{1100}$ .

for the  $\text{CuO}/\text{Al}_2\text{O}_3$  catalyst [5] but is lower than published by Norsk Hydro for the  $\text{Co}_2\text{AlO}_4/\text{CeO}_2$  catalyst (the  $\text{N}_2\text{O}$  conversion  $\sim 95\%$ ) [20] and Yara International  $\text{Co}_2\text{AlO}_4/\text{CeO}_2$  (the  $\text{N}_2\text{O}$  conversion over 80%) [24].

#### 4. Discussion

The Fe–Al catalysts showed high activity in the reaction of the  $\text{N}_2\text{O}$  decomposition at temperatures 700–800 °C and were

inactive in the NO decomposition at temperatures below 800 °C. The usefulness of catalysts for the nitrous oxide decomposition in the ammonia oxidation process gases and conditions depends on the influence of each of the mixture component ( $\text{O}_2$ , NO and  $\text{H}_2\text{O}$ ) on the catalyst activity. Known from literature [4,25], disadvantageous influence of the water vapour has been confirmed. However, the decrease in the activity of the catalysts, especially the most active ones, at the  $\text{H}_2\text{O}/\text{NO} = 3\text{--}6$  ratio is not significant (Fig. 5). The lack of

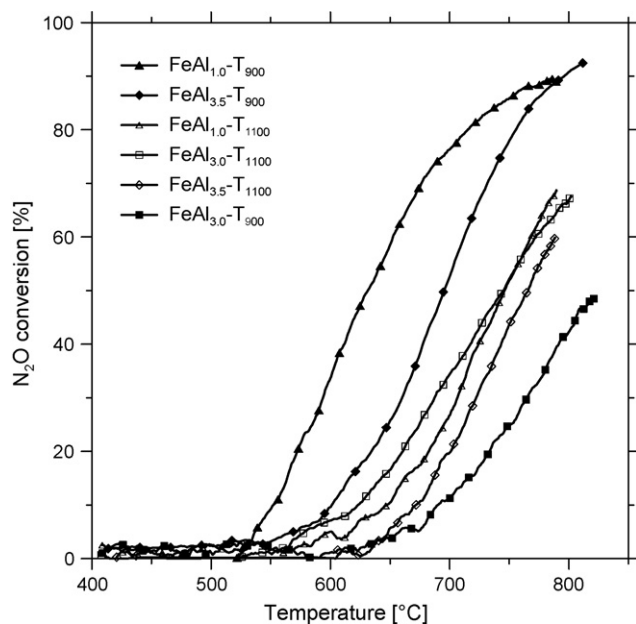


Fig. 4.  $\text{N}_2\text{O}$  conversion vs. temperature. Conditions:  $P = 1$  bar,  $F = 100$   $\text{cm}^3/\text{min}$ , 0.5 vol.% of  $\text{N}_2\text{O}$ , 0.5 vol.% of  $\text{O}_2$ , 3.0 vol.% of NO, balance He.

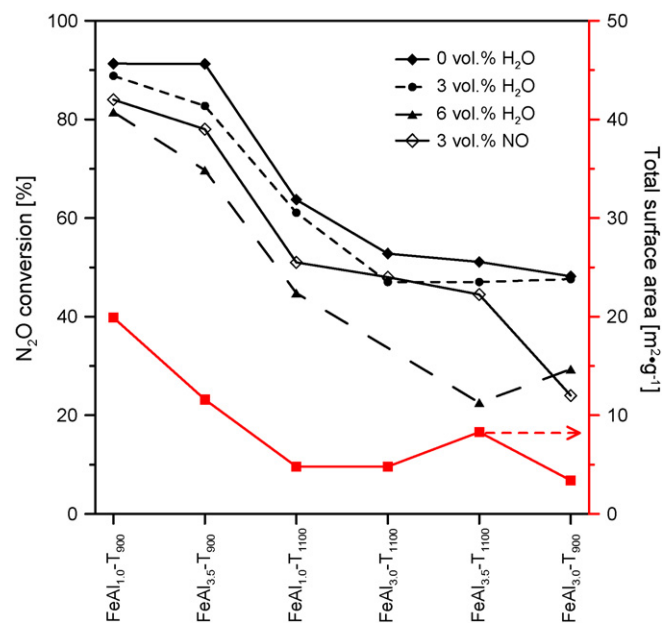


Fig. 5. Decomposition of  $\text{N}_2\text{O}$ , effect of concentration of water, NO and total surface area of the catalysts. Conditions:  $T = 750$  °C, atmospheric pressure,  $F = 100$   $\text{cm}^3/\text{min}$ , 1 vol.% of  $\text{N}_2\text{O}$ , 1 vol.% of  $\text{O}_2$ , balance He.



Fig. 6. Pilot plant reactors used to study oxidation of ammonia and decomposition of nitrous oxide.

the influence of the oxygen presence in the reaction mixture on the catalysts activity [5,26] has been also corroborated. The most controversial is the effect of the NO presence in the reaction mixture on the activity of the catalysts in  $N_2O$  decomposition.

A number of experimental studies by Pérez-Ramírez et al. [4,23,27] have shown that for the Fe–zeolites as well as for other Fe-based catalysts, NO significantly enhances their activity in the direct  $N_2O$  decomposition. The promotion effect of NO is larger for Fe–zeolites than for Fe-supported oxides [23] and it requires a low NO concentration in the feed with no significant improvements at the molar NO/ $N_2O$  feed ratio higher than 0.25 [27]. Since no NO inhibition at the molar NO/ $N_2O$  feed ratio of 10 was observed, the authors suggested

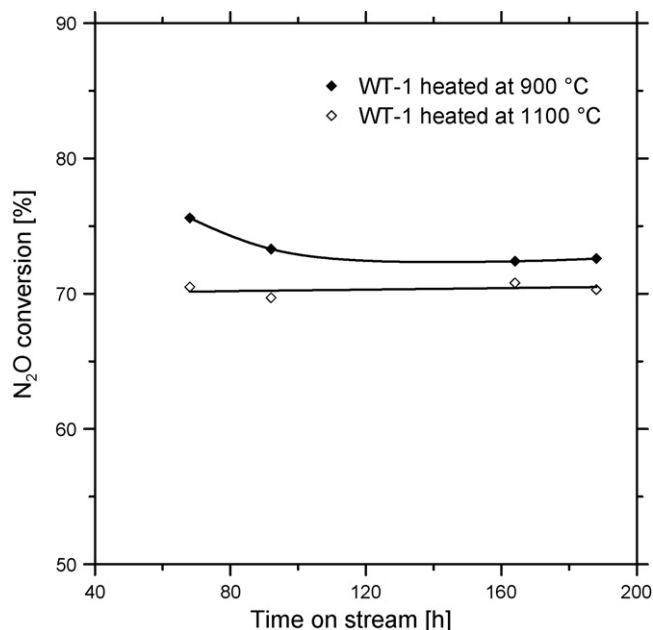


Fig. 7. Pilot plant studies for in-process-gas  $N_2O$  decomposition for WT-1 catalyst. Conditions:  $P = 4.9$  bars,  $T = 890$  °C,  $F = 45$  m<sup>3</sup>/min,  $NH_3$ :air = 10.7:89.3, v/v,  $N_2O = 1200$ –1300 ppm, the catalyst in the form of pellets.

different sites for NO adsorption and oxygen deposition by  $N_2O$  in Fe-ZSM-5. As a result they proposed the rate-determining step during the direct  $N_2O$  decomposition being the desorption of oxygen from the catalyst surface [27]. Novakova and Sobalik [28] confirmed these findings and reported that the promotional effect of NO depends not only on the NO/ $N_2O$  ratio, the temperature and the zeolite matrix but also on the type, location and the amount of the iron. Recently, Pirngruber et al. [12] confirmed that the surface migration and recombination of surface oxygen atoms to  $O_2$  is the rate-limiting step of the  $N_2O$  decomposition reaction on Fe–ZSM-5 zeolites. These authors reported that the nitrous oxide decomposition activity of Fe–ZSM-5 is strongly correlated with the autoreduction of the iron sites which decreases in the order: monomers, dimers > oligomers >  $Fe_2O_3$  particles [12]. However, as proved by Krishna and Makkee [29], the formation of different iron species is very sensitive to all of the catalyst preparation parameters, and even a small change in catalyst preparation or pretreatment procedure can lead to changes in the structure of active iron species and its relative distribution. Due to the high iron loading in the catalysts as well as their high temperature post-preparation treatment the nature of active sites is probably quite different than in zeolites. Recent studies on the Fe-Al catalysts for the Fisher-Tropsch synthesis [30] or selective catalytic reduction of N-containing compounds [31] suggested the presence of the  $Fe_2O_3$  particles as a main phase in the catalysts. According to the results presented by Fujimura et al. [32], high temperature treatment of the Fe/ $Al_2O_3$  samples in air leads to the formation of  $\alpha$ - $Fe_2O_3$  and  $FeAl_2O_4$  phase. These findings confirmed our TPR and XRD experiments conclusions about the nature of the iron species on the surface of the catalysts. Our activity results showed that nitric oxide does not promote the  $N_2O$  decomposition. This could indicate, that the reaction mechanism for the  $N_2O$  decomposition is independent of NO, which has been already reported by Heyden et al. [33]. However, the presence of NO surprisingly inhibits the nitrous oxide decomposition reaction on the FeAl catalysts. Very high iron loading in the catalysts comparing to the Fe–zeolites leads to the formation of  $Fe_2O_3$  particles, oligonuclear and cluster iron species which do not autoreduce easily, so the fraction of iron sites taking part in the catalytic cycle is much smaller [12]. The negative effect of NO can then be explained by the competitive adsorption of NO on the small amount of  $N_2O$  decomposition active sites. This assumption can be authenticated by the comparison of activity results with the total surface area of the catalysts (Fig. 5). Ramis and Angeles Larrubia [31] suggested that during the NO adsorption on the  $Fe_2O_3/Al_2O_3$  catalyst nitrous oxide can be formed what could also decrease the overall  $N_2O$  conversion level. Moreover the NO in the reaction mixture can be adsorbed on the alumina surface forming a number of different transformation species [31,34]. The most resistant for the reaction mixture composition (i.e.  $H_2O$  and NO presence) is the catalyst with the highest total surface area thus the highest amount of nitrous oxide decomposition active sites. However, this assumption has to be confirmed by the further studies on the properties of the catalysts surface iron

species. Therefore, the preparation method and catalysts composition play a significant role in the activity of the  $\text{Fe}_2\text{O}_3/\text{Al}_2\text{O}_3$  catalysts.

## 5. Conclusions

The decomposition of  $\text{N}_2\text{O}$  on  $\text{Fe}_2\text{O}_3/\text{Al}_2\text{O}_3$  catalysts in the simulated nitric acid production process stream was investigated. The most active catalysts exhibited high activity in the nitrous oxide decomposition at temperatures over  $750^\circ\text{C}$  and from the other side they were inactive in the NO decomposition up to  $800^\circ\text{C}$ . The  $\text{N}_2\text{O}$  decomposition activity was strongly correlated with the total surface area of the samples thus the catalyst composition, preparation method and post-preparation temperature treatment conditions. The presence of  $\text{H}_2\text{O}$  as well as NO decreases the nitrous oxide conversion. The usefulness of the catalysts to decompose  $\text{N}_2\text{O}$  in the nitric acid production plant was confirmed by the results of the 180 h pilot-plant and 3300 h real-plant experiments. During these experiments nearly no decrease in the catalysts activity or the mechanical stability were stated and the achieved nitrous oxide abatement level was sufficient to fulfill the future EU environmental norms.

## Acknowledgment

This work was supported by the Vice Rector for Science and Research of the University of Maria Curie-Skłodowska as an individual research project.

## References

- [1] Inventory of US Greenhouse Gas Emissions and Sinks: 1990–2005, U.S. EPA, Washington, 2007.
- [2] R.W. van den Brink, S. Booneveld, J.R. Pels, D.F. Bakker, M.J.F.M. Verhaak, *Appl. Catal. B* 32 (2001) 73.
- [3] Market analysis  $\text{DeN}_2\text{O}$ . Market potential for reduction of  $\text{N}_2\text{O}$  emissions at nitric acid facilities, Jacobs Engineering Nederland, Leiden, 2001.
- [4] J. Pérez-Ramírez, F. Kapteijn, G. Mul, X. Xu, J.A. Moulijn, *Catal. Today* 76 (2002) 55.
- [5] J. Pérez-Ramírez, F. Kapteijn, K. Schöffel, J.A. Moulijn, *Appl. Catal. B* 44 (2003) 117.
- [6] F. Kapteijn, J. Rodríguez-Mirasol, J.A. Moulijn, *Appl. Catal. B* 9 (1996) 25.
- [7] J. Pérez-Ramírez, A. Gallardo-Llamas, *J. Catal.* 223 (2004) 382.
- [8] I. Melián-Cabrera, C. Mentrut, J.A.Z. Pieterse, R.W. van der Brink, G. Mul, F. Kapteijn, J.A. Moulijn, *Catal. Commun.* 6 (2005) 301.
- [9] A. Ates, A. Reitzmann, *J. Catal.* 235 (2005) 164.
- [10] T. Nobukawa, K. Sugawara, K. Okumura, K. Tomishige, K. Kunimori, *Appl. Catal. B* 70 (2007) 342.
- [11] B.R. Wood, J.A. Reimer, A.T. Bell, M.T. Janicke, K.C. Ott, *J. Catal.* 224 (2004) 148.
- [12] G.D. Pirngruber, P.K. Roy, R. Prins, *J. Catal.* 246 (2007) 147.
- [13] M.A.G. Hevia, J. Pérez-Ramírez, *Appl. Catal. B* 77 (2007) 248.
- [14] T. Nobukawa, M. Yoshida, K. Okumura, K. Tomishige, K. Kunimori, *J. Catal.* 229 (2005) 374.
- [15] M. Baier, T. Fetzner, O. Hofstadt, M. Hesse, G. Bürger, K. Harth, V. Schumacher, H. Wistuba, B. Otto, WO 00/23176, 2001, to BASF.
- [16] P.D. VerNooy, US 6,379,640 B1, 2002, to E.I. du Pont.
- [17] P.D. VerNooy, US 6,710,010 B2, 2004, to E.I. du Pont.
- [18] M. Schwefer, WO 01/58570, 2001, to UHDE.
- [19] G. Delahay, M. Mauvezin, B. Neveu, G. Neveu, B.M. Coq, US 6,890,501 B2, 2005, to Engelhard.
- [20] Ø. Nirisen, K. Schöffel, D. Waller, D. Øvrebø, WO 02/02230 A1, 2002, to Norsk Hydro.
- [21] M.J. Tiernan, P.A. Barnes, G.M.B. Parkes, *J. Phys. Chem. B* 105 (2001) 220.
- [22] D.B. Bukur, K. Okabe, M.P. Rosynek, C. Li, D. Wang, K.R.P.M. Rao, G.P. Huffman, *J. Catal.* 155 (1995) 353.
- [23] J. Pérez-Ramírez, F. Kapteijn, G. Mul, J.A. Moulijn, *J. Catal.* 208 (2002) 211.
- [24] T. Kopperud, *Platinum Met. Rev.* 50 (2) (2006) 103.
- [25] D.A. Bulushev, P.M. Precht, A. Renken, L. Kiwi-Minsker, *Ind. Eng. Chem. Res.* 46 (2007) 4178.
- [26] F. Kapteijn, G. Marbán, J. Rodríguez-Mirasol, J.A. Moulijn, *J. Catal.* 167 (1997) 256.
- [27] J. Pérez-Ramírez, G. Mul, F. Kapteijn, J.A. Moulijn, *Kinet. Katal.* 44 (2003) 639.
- [28] J. Novakova, Z. Sobalik, *Catal. Lett.* 111 (2006) 195.
- [29] K. Krishna, M. Makkee, *Catal. Lett.* 106 (2006) 183.
- [30] H.J. Wan, B.S. Wu, Ch.H. Zhang, H.W. Xiang, Y.W. Li, B.F. Xu, F. Yi, *Catal. Commun.* 8 (2007) 1538.
- [31] G. Ramis, M. Angeles Larrubia, *J. Mol. Catal. A: Chem.* 215 (2004) 161.
- [32] T. Fujimura, S.-I. Tanaka, *J. Mater. Sci.* 34 (1999) 425.
- [33] A. Heyden, N. Hansen, A.T. Bell, F.J. Keil, *J. Phys. Chem. B* 110 (2006) 17096.
- [34] T. Venkov, K. Hdjivanov, D. Klissursky, *Phys. Chem. Chem. Phys.* 4 (2002) 2443.